Full geroprotection from brief rapamycin treatment by persistently increased intestinal autophagy

Paula Juricic[1,2]†, Yu-Xuan Lu[1]†, Thomas Leech[1]†, Lisa F. Drews[1], Jonathan Paulitz[1], Jiongming Lu[1], Tobias Nespital[1], Sina Azami[1], Jennifer C. Regan[3,4], Emilie Funk[1], Jenny Fröhlich[1], Sebastian Grönke[1], Linda Partridge[1,4*]

[1]Max Planck Institute for Biology of Ageing, Cologne, Germany.

[2]Present address: Lunaphore Technologies SA, Tolochenaz, Switzerland.

[3]Present address: University of Edinburgh, Institute of Immunology and Infection Research, Edinburgh, UK.

[4]Institute of Healthy Ageing, and Department of Genetics, Evolution and Environment, UCL, London, UK.

†These authors contributed equally

*Correspondence to: Linda.Partridge@age.mpg.de

Abstract

The licensed drug rapamycin has potential to be repurposed for geroprotection. A key challenge is to avoid adverse side-effects from continuous dosing regimes. Here we show a profound memory effect of brief, early rapamycin treatment of adults, which extended lifespan in *Drosophila* to the same degree as lifelong dosing. Lasting memory of earlier rapamycin treatment was mediated by elevated autophagy in enterocytes of the gut, accompanied by increased intestinal lysosomal alpha-mannosidase V (LManV) and lysozyme levels and improved structure and function of the ageing intestine. Brief elevation of autophagy itself induced a long-term increase in autophagy. In mice, a short-term, 3-month treatment in early adulthood also induced a memory effect, with enhanced autophagy in Paneth cells, improved Paneth cell

architecture and gut barrier function at levels induced by chronic treatment, even 6 months after rapamycin was withdrawn. Past rapamycin treatment also enhanced the regenerative potential of aged intestine in intestinal organoids. Full geroprotective effects of chronic rapamycin treatment can thus be obtained with a brief pulse of the drug.

Main

The macrolide drug rapamycin inhibits TORC1 activity and can extend lifespan in model organisms, including mice[1-3]. In mice rapamycin can delay several age-related diseases, such as cognitive decline[4], spontaneous tumours[5], and cardiovascular[6,7] and immune dysfunction[8]. However, chronic rapamycin administration can cause adverse effects, even with low doses[9,10]. Shortening treatment could potentially reduce negative effects. Short-term treatment in late life can extend lifespan in mice[3,11,12] and enhance immune response in elderly humans[13,14]. However, it is unknown whether the effects of late-life treatment are comparable to those of lifelong drug exposure, or whether brief treatment at younger ages is sufficient to gain the full benefits of chronic treatment.

To assess the efficacy of late-onset rapamycin treatment, we treated *Drosophila* at different ages and for varying durations. Treatments starting later in life, on day 30 or day 45, extended lifespan, consistent with previous findings in mice[3,11,12], but less than did lifelong treatment (Extended Data Fig. 1a-b, and Table 1 and 2). Very late-onset rapamycin treatment from day 60, when survival is already decreased to ~80%, did not increase lifespan (Extended Data Fig. 1c and Table 1). Thus, later onset rapamycin treatment produced progressively smaller extensions of lifespan.

1   In sharp contrast, rapamycin treatment instigated early in adulthood on day 3 following

2   eclosion and 2 days of mating (termed "day 1"), for just 30 days, extended lifespan as much as

3   did lifelong dosing (Extended Data Fig. 1d and Table 2). Treatment from day 15-30 increased

4   lifespan, but less than did chronic treatment (Extended Data Fig. 1e and Table 3). Remarkably,

5   rapamycin in only the first 15 days of adult life recapitulated the full lifespan extension

6   achieved by chronic treatment (Fig. 1a and Extended Data Table 3), a phenomenon we termed

7   'rapamycin memory'.

8

9   Rapamycin increases lifespan mainly in female *Drosophila* [2]. The number of dividing intestinal

10   stem cells (ISCs) increases with age in female flies, to restore damaged parts of the intestinal

11   epithelium, driving intestinal dysplasia later in life[15]. Thus, we hypothesized that short-term

12   rapamycin might permanently alter ISC activity. As previously reported[16], chronic rapamycin

13   treatment reduced pH3+ cell number (Fig. 1c), a marker for dividing cells[17]. Strikingly, the

14   number of pH3+ cells of flies treated with rapamycin only during days 1-15 remained as low as

15   in flies treated chronically, even 10, 30 and 45 days post-treatment (Fig. 1b-c; Extended Data

16   Fig. 2a-b). Mass spectrometry confirmed that rapamycin concentration was reduced to the level

17   of control flies 10-days after rapamycin treatment on days 1-15 was ended (Extended Data Fig.

18   2c). The ISCs thus remained fully quiescent long after rapamycin was withdrawn.

19

20   We next assessed the turnover rate of the intestinal epithelium using the *esg^{ts}* F/O system (esg-

21   *Gal4; tubGal80^{ts} Act>CD2>Gal4 UAS-Flp UAS-GFP)*[18], where activation by a temperature shift to

22   29°C marks ISCs and their progenitor cells with GFP. Under standard conditions, the epithelial

3

1   turnover rate in *Drosophila* is 14 days. Temperature increase shortens lifespan, so we measured

2   turnover rate 10 and 20 days post-treatment. Most of the control midgut epithelium was

3   replaced by GFP positive cells after 10 (Extended Data Fig. 2d) and 20 days (Fig. 1d) of system

4   activation. Chronic and day 1-15 rapamycin treatment reduced the number of GFP positive cells

5   10 and 20 days after the switch to the same extent (Fig. 1d; Extended Data Fig. 2d). Brief, early

6   rapamycin exposure thus reduced turnover of the intestinal epithelium as much as chronic

7   treatment, and the cells previously treated with rapamycin remained in the gut until advanced

8   age.

9

10   Staining with diphosphorylated Erk (dpErk), a specific readout for signal that damaged and

11   apoptotic enterocytes send to the ISCs for replacement[19], revealed that short-term rapamycin

12   treatment reduced the number of apoptotic, dpErk positive cells as much as did chronic

13   treatment (Fig. 1e), suggesting increased enterocyte health. We therefore assessed if intestinal

14   pathologies were reduced. Histology using the epithelial marker *Resille-GFP* revealed that

15   dysplastic regions were widespread throughout the gut of ageing control flies (Fig. 1f). Flies

16   treated chronically or from days 1-15 with rapamycin had significantly fewer dysplastic lesions

17   even 45 days after rapamycin was withdrawn (Fig. 1f). Since lifespan is directly linked to gut

18   barrier function, and loss of septate-junction proteins disrupts gut integrity[20], we measured the

19   effect of brief rapamycin treatment on gut barrier function. Intestinal integrity, as measured by

20   a blue dye leakage assay, was preserved by rapamycin treatment and remained protected even

21   45 days after rapamycin was withdrawn (Fig. 1g). Taken together, these results indicate that

22   brief, early-life rapamycin exposure exerted long-lasting protective effects on the intestine by

4

1   reducing turnover of the epithelium, and preventing age-related increase in ISC proliferation,

2   dysplasia and loss of intestinal barrier function.

3

4   Persisting effects of brief rapamycin treatment could indicate a persistent inhibition of TORC1

5   activity. S6K is a direct target of TORC1 and reduced phosphorylation of S6K is required for

6   extension of lifespan by rapamycin[2]. Rapamycin treatment instigated later in life, on day 30,

7   reduced TORC1 activity within 48 hours to the same level as chronic treatment in head, muscle,

8   fat body and gut (Extended Data Fig. 3a-d). In contrast to lifespan, terminating rapamycin

9   treatment on day 30 de-repressed TORC1 activity to the level of control flies in all four tissues

10   (Extended Data Fig. 3a-d). In accordance with the absence of a 'memory effect' for intestinal

11   S6K phosphorylation, over-expression of constitutively active S6K in the gut did not abolish

12   lifespan extension by chronic or short-term rapamycin treatment (Extended Data Fig. 3e-f and

13   Extended Data Table 4). Thus, TORC1 activity responded acutely to rapamycin, and events

14   downstream of TORC1 other than reduced activity of S6K in the intestine, induced the

15   'rapamycin memory' effects.

16   Increased autophagy is also a downstream effector of TORC1, and is required for lifespan

17   extension by rapamycin[2]. Persistently up-regulated autophagy could therefore carry the

18   'memory of rapamycin'. To assess autophagic flux, we performed co-staining with Cyto-ID and

19   lysotracker dye. While Cyto-ID specifically labels autophagosomes, lysotracker stains

20   autolysosomes, and an increased ratio of autolysosomes to autophagosomes indicates

21   increased autophagic flux [21]. Chronic rapamycin treatment increased levels of autolysosomes,

22   without altering the levels of autophagosomes, indicative of an increased autophagic flux (Fig 2.

5

1   a). Strikingly, the number of LysoTracker-stained punctae remained fully elevated even 10-days

2   (Fig. 2a) and 30-days (Extended Data Fig. 4a) after rapamycin was withdrawn, with no change in

3   Cyto-ID positive punctae (Fig. 2a). Immunoblot analysis revealed that chronic treatment

4   decreased the levels of intestinal, non-lipidated and lipidated forms of the Atg8 protein and the

5   *Drosophila* p62 homolog Ref-2-P and these stayed low 10-days after the treatment from day 1-

6   15 was withdrawn (Fig. 2b), indicative of persistently activated autophagy. However, rapamycin

7   had no effect on Atg8 and Ref-2-P in heads (Extended Data Fig. 4b), suggesting a tissue-specific

8   response. Together, these results suggest that autophagy induced by brief rapamycin treatment

9   stayed induced for a prolonged period after rapamycin was withdrawn, despite TORC1 activity

10   being restored back to control levels within 48 hours.

6

To test for a causal role of elevated autophagy in the intestine in the 'rapamycin memory', we abrogated it, both briefly and chronically, with double stranded RNA interference. We used inducible GeneSwitch drivers to drive expression of *Atg5*-RNAi in intestinal stem cells (ISCs) or enterocytes. Surprisingly, chronic and day 1-15 treatment with rapamycin both failed to increase lifespan of flies expressing *Atg5*-RNAi specifically in enterocytes (Fig. 2c, Extended Data Fig. 5a and Table 5), but not in ISCs (Extended Data Fig. b-c and Table 6). Furthermore, enterocyte-specific chronic and day 1-15 over-expression of *Atg5*-RNAi abrogated protection of gut barrier function by chronic and brief rapamycin exposure, respectively (Fig. 2d and Extended Data Fig. 5d). Blocking the increase in autophagy in response to rapamycin in the enterocytes of the gut thus completely abolished the 'rapamycin memory' effect on both lifespan and intestinal integrity.

To determine whether direct, genetic activation of autophagy was sufficient to mimic the 'memory of rapamycin' in the absence of the drug, we over-expressed *Atg1*, which induces autophagy in flies[22]. Interestingly, similar to rapamycin short-term treatment, over-expression of *Atg1* in enterocytes from days 1-15 caused lasting down-regulation of Ref-2-P 10 days after *Atg1* over-expression was terminated (Fig. 2e). Combining rapamycin with enterocyte-specific over-expression of *Atg1* from days 1-15 did not further reduce Ref-2-P levels (Fig. 2e). Furthermore, lifelong and day 1-15 enterocyte-specific over-expression of *Atg1* extended lifespan (Fig. 2f and Extended Data Fig. 6a) and prevented age-related loss of intestinal integrity (Fig. 2g and Extended Data Fig. 6b) as much as did chronic or brief rapamycin exposure, and the

1   combination of *Atg1* over-expression and rapamycin did not further increase lifespan (Fig. 2f

2   and Extended Data Fig. 6a and Table 7) or improve gut barrier function (Fig. 2g and Extended

3   Data Fig. 6b). Thus, brief elevation of autophagy in enterocytes induces a memory identical to

4   that from brief rapamycin treatment, and mediates the 'memory of rapamycin' in increased

5   autophagy, intestinal health and lifespan.

6

7   To test whether the recently reported rapamycin-mediated increase in histone expression [21]

8   underlies rapamycin memory, we investigated histone H3 expression after d1-15 rapamycin

9   treatment and the effects of over-expression of H3/H4 during d1-15 on autophagy, gut health

10   and lifespan. As expected, H3 expression was induced by chronic rapamycin treatment, but was

11   decreased back to control levels 15 days post-treatment. Moreover, although chronic over-

12   expression of H3/H4 extended lifespan, decreased pH3+ cell count, accumulation of chromatin

13   at the nuclear envelope and intestinal dysplasia and increased lysotracker staining, these

14   phenotypes showed no memory of previous d1-15 H3/H4 expression (Extended data Fig. 7).

15   These data suggest that, although increased histone expression mediates lifespan extension by

16   chronic rapamycin treatment, this mechanism is distinct from the one that is responsible for

17   the memory of short-term rapamycin treatment.

18

19   To search for regulators of the 'memory effect' of rapamycin and elevated autophagy, we

20   performed proteomics analysis. Gene ontology (GO) term enrichment analysis of the proteins

21   that were increased by rapamycin treatment on day 25 and that remained induced 10 days

22   after the treatment revealed high enrichment in proteins involved in carbohydrate metabolism,

1   in particular lysosomal mannosidases (Extended Data Fig. 8). We confirmed the increase in

2   lysosomal alpha-mannosidase V (LManV) mRNA levels by qRTPCR (Extended Data Fig. 9). We

3   therefore tested if knock-down of LManV abolished the 'memory of rapamycin'. Indeed, knock-

4   down of LManV blocked both the increase in lysotracker-stained punctae by rapamycin

5   treatment during days 1-15 (Fig 3a) and the improved gut pathology mediated by short-term

6   rapamycin treatment (Fig 3b). To test if LManV activation was sufficient to mimic short-term

7   rapamycin treatment, we over-expressed LManV during days 1-15, and found that it increased

8   lysotracker-stained punctae and reduced age-related gut pathologies to the same degree as

9   chronic over-expression of LManV (Fig 3c-d). Taken together these findings suggest that the

10   'memory of rapamycin' in elevated autophagy and improved gut health is mediated through

11   increased expression of LManV.

12   Recent studies showed that lysozyme-associated secretory autophagy plays a key role in gut

13   health and pathogenesis in mammalian small intestine [23,24]. Secretory autophagy is an

14   autophagy-based alternative secretion system that is activated in response to infection, and it is

15   mediated by core autophagy proteins Atg5 and Atg16L1. Based on our data suggesting the

16   importance of autophagy in the gut for the "memory of rapamycin", we assessed whether

17   levels of intestinal lysozyme, as a proxy for secretory autophagy, were affected by rapamycin

18   treatment. We found that they were increased, and remained so 10 days after the treatment

19   was withdrawn. These responses to rapamycin were unaffected by tetracycline treatment (Fig

20   3e), suggesting that the intestinal microbiota did not play a role. To investigate if LManV and

21   autophagy were responsible for inducing increased lysozyme, we measured lysozyme in

22   intestines of flies over-expressing LManV, and found that both chronic and short-term over-

expression increased lysozyme levels to the same degree. Knock-down of LManV by RNAi partially abolished increased lysozyme by rapamycin treatment in days 1-15 (Fig 3f-g), while blocking autophagy by RNAi against Atg5 abolished the increase in lysozyme induced by d1-15 rapamycin treatment (Fig 3h). Together, these data suggest that autophagy and LManV mediate rapamycin-induced increase in intestinal lysozyme.

To assess if lasting benefits of a short-term rapamycin treatment are conserved between flies and mammals, we assessed the impact of rapamycin treatment on intestinal permeability in mice, by measuring plasma lipopolysaccharide-binding protein (LBP) levels, a marker of bacterial translocation from intestine into circulation[25,26]. As we (Fig 4b) and others[27] showed that the age-related increase in gut permeability in rodents appears already in middle-age, we treated mice with rapamycin chronically or from 3-6 months of age, and collected samples 6 months after the treatment was withdrawn, at 12-months of age (Fig. 4a). Strikingly, 6 months after rapamycin was withdrawn plasma LBP levels were reduced to levels similar to those with chronic treatment, (Fig. 4b), suggesting that the long-lasting, beneficial effects of short-term rapamycin exposure on intestinal integrity is conserved in mammals.

Increased gut permeability is associated with compromised tight junctions (TJ)[28]. Irregularities of TJ can be observed by electron microscopy as reduced electron density of the perijunctional ring[29] and dilations within tight junctions[30]. We analyzed ultrastructure of TJs in jejunal villi. Intact TJs, which appeared as narrow and electron-dense structures, were classified as class I, narrow TJs with reduced electron density, but without dilations within the TJ as class II, and TJs that were both low in electron density and dilated as class III (Fig 4c). In line with previously

1   published data on gut permeability [27], TJ quality declined during ageing, with 7 month old mice

2   already showing reduced proportion of intact TJs compared to 3 month old mice (Fig 4c). In

3   accordance with plasma LBP result, rapamycin treatment increased the proportion of intact TJs,

4   which remained increased 6 months after rapamycin withdrawal, further supporting the

5   hypothesis that rapamycin protects age-related decline in intestinal integrity (Fig 4c and

6   Extended Data Fig. 10).

7   Paneth cells are specialized secretory cells that serve as a niche for ISCs[31] and contain secretory

8   granules filled with antimicrobial proteins, such as lysozyme, and rapamycin improves the

9   Paneth cell function and their support of ISCs[32]. Lysozyme is normally efficiently packed in

10   Paneth cell granules[23]. In 12 months-old control mice, we observed a notable proportion of

11   Paneth cells with abnormal lysozyme distribution, which was diffuse in cells. Short-term

12   rapamycin treatment increased the proportion of cells with lysozyme packed granules and

13   reduced those with a diffuse lysozyme signal (Fig. 4d). Transmission electron microscopy

14   further showed that Paneth cell granule abnormalities, seen as loosely packed and hypodense

15   granules that are a feature of dysfunction[23], appeared already at 12 months of age (Fig. 4e).

16   Remarkably, rapamycin treatment decreased the proportion of hypodense Paneth cell granules,

17   which stayed decreased to the levels seen with chronic treatment 6 months after rapamycin

18   treatment was withdrawn (Fig. 4e). Together, these data suggest that short-term rapamycin

19   treatment abolished age-related Paneth cell abnormalities[23].

20   Next, we assessed if the long-term elevation of autophagy by past rapamycin treatment is

21   conserved in mice. Although chronic and 3-6 months rapamycin treatment did not significantly

11

1   reduce the number of p62 punctae in the villi region, comprising enterocytes and goblet cells,

2   there was a trend in the villi of 12 months old rapamycin treated mice (Extended Data Fig. 11).

3   As autophagy is essential for proper Paneth cell function and secretion[23], and upon autophagy

4   activation autophagy-related proteins colocalize with Paneth cell granules[33], we measured the

5   number of granules positive for both lysozyme and p62. Chronic and 3-6 months rapamycin

6   treatment increased the number of Paneth cell granules positive for both lysozyme and p62

7   assessed at 12 months of age (Fig. 4f), suggesting that autophagy in Paneth cells remained

8   induced 6 months after rapamycin treatment was withdrawn, allowing proper Paneth cell

9   secretion.

10   As we showed that LManV is one of the mediators of rapamycin memory in *Drosophila*, and

11   that it also mediates rapamycin-induced increase in lysozyme levels in flies, we measured the

12   levels of mannosidases in mouse gut. We observed that rapamycin increased the number of

13   Man2B1 positive punctae in intestinal crypts, and these stayed increased 6 months after the

14   treatment was withdrawn (Fig 4g), in line with the fly data.

15   During ageing, regenerative capacity of the intestinal epithelium, measured as the ability of ISC-

16   containing epithelial crypts to form clonogenic organoids, declines due to defects in both ISC

17   and Paneth cells[34]. To elucidate whether short-term rapamycin treatment could abolish age-

18   related decline in organoid-forming potential, we treated mice with rapamycin starting from

19   15-21 months of age, followed by a switch to control food for another 2 months (Fig. 4h).

20   Strikingly, short-term treatment increased organoid forming potential of intestinal crypts

21   isolated 2 months after drug withdrawal (Fig. 4i). Importantly, regenerative growth of de novo

12

crypts was also increased in organoids generated from intestines from pre-treated mice (Fig. 4j).

Together, these data show that short-term rapamycin exposure in adult mice combated age-related declines in intestinal TJ structure, Paneth cell architecture, gut barrier and regenerative capacity of ISC and Paneth cells, and that these geroprotective effects were equivalent to those seen with chronic drug exposure and lasted long after rapamycin treatment was withdrawn.

Our study has uncovered a long-lasting effect of short-term rapamycin administration, including prolonged activation of autophagy, reduced age-related gut pathologies and extension of lifespan. Brief rapamycin administration in early adult life induced these benefits to the same degree as lifelong treatment, with a key role of the enterocytes in the intestine. The long-term elevation in autophagy was mediated by the lasting increase in LManV expression. These findings are intriguing in light of the key role of autophagy in an array of age-related diseases, including cancer[35], immune system dysfunction[8], and neurodegenerative diseases[36]. Our findings suggest that the full geroprotective effects of rapamycin can be achieved without the adverse effects sometimes seen with chronic, long-term dosing. It will be important to determine the temporal clinical dosing regimen that maximizes protection while minimizing side-effects.

1 **Methods**

2 Fly husbandry and strains

3 The white *Dahomey* (w[Dah]), *Wolbachia* positive strain was used, unless otherwise stated.

4 Fly stocks were maintained at 25°C on a 12 h light/dark cycle, at constant humidity (60%), and

5 reared on sugar/yeast/agar (SYA) diet, at standard larval density, by collecting eggs on grape

6 juice plates, washing with PBS and pipetting 20 μl of the eggs into each culture bottle. Eclosing

7 adult flies were collected over 18 h and mated for 48 hours, then sorted into single sexes.

8 Female flies were used. All mutants and transgenes were backcrossed for at least six

9 generations into the w[Dah] background. The following strains were used in the study: *TiGS* [37],

10 *5966GS* [38], *5961GS* [15,39], *Resille-GFP* from the Flytrap project[40], *UAS-Atg5*-RNAi and *UAS-Atg1* OE

11 (GS10797) obtained from the Kyoto Drosophila Genetic Resource Center [41,42], *UAS-LManV* [43],

12 *UAS-LManV RNAi* (GD13040) obtained from Vienna Drosophila Stock Center, *UAS-H3/H4* were

13 generated in this lab [21].

14

15 Standard media and rapamycin treatment for *Drosophila*

16 Standard SYA medium was used, containing per liter (L) 100 g autolyzed yeast powder

17 (brewer's yeast, MP Biomedicals), 50 g sucrose (Sigma), 15 g agar (Sigma), 3 ml propionic acid

18 (Sigma), 30 ml Nipagin (methyl 4-hydroxybenzoate) and distilled water to 1 L. SYA diet was

19 prepared as described before[44]. Rapamycin was dissolved in ethanol, and added to the food in

20 concentration of 200 μM.

21

14

1   **Lifespan assays**

2   Females were placed into vials containing experimental diets and drugs, at a density of 20

3   flies/vial, and transferred into vials containing fresh food every 2-3 days, when the number of

4   dead flies was scored. Sample size and analyses of all lifespan data are shown in Extended Data

5   Tables 1-7.

6

7   **Mouse husbandry and rapamycin treatment**

8   Female C3B6F1 hybrids were used and were bred in an in-house animal facility at the Max

9   Planck Institute for Biology of Ageing. C3B6F1 hybrids were generated by a cross between C3H

10   female and C57BL/6J male mice, obtained from Charles River Laboratories. Four-week-old mice

11   were housed in individually ventilated cages, in groups of five mice per cage, under specific-

12   pathogen-free conditions. Mice had *ad libitum* access to chow (Ssniff Spezialdiäten GmbH; 9%

13   fat, 24% protein, 67% carbohydrates) and drinking water at all times. Experiments were

14   conducted under the approval of the State Office for Nature, Environment and Consumer

15   Protection North Rhine-Westphalia (approval nos. 84-02.04.2017.A074 and 84-

16   02.04.2015.A437). For 6-months post-switch measurements, rapamycin was added at

17   concentration of 14 ppm (mg of drug per kg of food), encapsulated in Eudragit S100 (Evonik).

18   Control chow contained Eudragit encapsulation medium only. Rapamycin treatment was

19   initiated at 3 months of age and was administered either continuously until 12-months of age

20   (rapamycin chronic group) or until month 6, after which the switch-off group received control

21   chow for an additional 6 months (rapamycin 3-6M group). All mice from 6-months-post-switch-

22   experiment were sacrificed at 12 months of age. For the 2-month post-switch organoid

1   experiment, rapamycin treatment (42 ppm, -week-on/1-week-off intervals) was started at 15

2   months of age and terminated at 21 moths of age, after which switch-off group received

3   control chow for an additional 2 months. Mice were sacrificed at 23 months of age and 2

4   months post-treatment.

5

6   Western blot analysis

7   Tissues were lysed in 2xLaemmli buffer (head, thorax and fat body) and proteins

8   denatured at 95°C for 5 min. Proteins from gut were extracted using in 20% trichloric acid,

9   washed in 1 M Tris buffer (not pH'd), resuspended in 2xLaemmli buffer and denatured at 95°C

10   for 5 min. Proteins (10 μg) were separated using pre-stained SDS-PAGE gels (Bio-Rad) and wet-

11   transferred onto 0.45 μm nitrocellulose membrane (GE Healthcare). Blots were incubated with

12   primary p-T389-S6K (CST, 9209), S6K[2], Atg8 and Ref-2-P[45] antibodies. Appropriate HRP-coupled

13   secondary antibodies (ThermoFisher) were used. Signal was developed using ECL Select

14   Western Blotting Detection Reagent (GE Healthcare). Images were captured using

15   ChemiDocImager (Bio-Rad) and band intensity was analyzed using ImageJ.

16

17   Immunostaining of fly intestines

18   Flies were immobilized on ice and guts were dissected in ice-cold PBS. Dissected guts were

19   immediately fixed in 4% formaldehyde for 30 min, washed in 0.2% Triton-X / PBS (PBST) and

20   blocked in 5% bovine serum albumin (BSA) / PBS for 1 h on a shaker. Gut tissues were

21   incubated with primary pH3 (CST, 9701; 1:500), dpErk (CST, 4370;1:400) or lysozyme

22   (ThermoFisher Scientific, PA5-16668; 1:100) solutions in 5% BSA overnight at 4°C, followed by

16

1   incubation in secondary Alexa Fluor 594⊠donkey anti-rabbit antibody (ThermoFisher Scientific,

2   A21207; 1:1000). Guts were mounted in mounting medium containing DAPI (Vectashield,

3   H1200), scored and imaged using a Leica inverted microscope for the cell division assay and

4   confocal SP8-DLS for the dpErk staining. pH3 and dpErk imaging was done on the R2 region

5   proximal to proventriculus and for each intestine 3 adjacent images were taken.

6

7   Gut turnover assay

8   w^{Dah} were crossed to the esg^{ts} F/O flies (w; esg-Gal4, tubGal80^{ts}, UAS-GFP; UAS-flp,

9   Act>CD2>Gal4). Crosses were maintained and progeny were raised at 18°C. Following a 3-day

10   mating at 18°C, female flies were distributed into vials containing EtOH or rapamycin and kept

11   at 18°C for 15 days. On day 15, a subgroup of flies was switched from rapamycin to EtOH food

12   and all experimental groups were transferred to 29°C. Flies were maintained at 29°C for 10 and

13   20 days, after which guts were dissected, fixed in 4% formaldehyde, and mounted in DAPI-

14   containing mounting medium (Vectashield, H1200). Samples were imaged under a confocal

15   microscope (Leica TCS SP8-X), and images analyzed using ImageJ. The GFP-marked regions

16   represent ISCs and their newly generated progenitor cells, and the GFP-marked area compared

17   to the total corresponding gut area indicates the gut turnover rate. Images were obtained from

18   R4 and R5 intestinal regions.

19

20   Gut barrier analysis

21   Flies were aged for 65 days on standard SYA diet then transferred into vials containing SYA

22   food with 2.5 % (w/v) FD&C blue dye no. 1 (Fastcolors). The proportion of blue (whole body is

17

1   blue) or partially blue (at least 2/3 of body is blue) flies was scored 24 h after exposure to the

2   blue food.

3

4   ## Imaging of gut dysplasia

5   Guts were dissected in ice-cold PBS, fixed in 4% formaldehyde for 30 min and mounted in

6   DAPI-containing mounting medium (Vectashield, H1200). Endogenous GFP and DAPI were

7   imaged using a confocal microscope. For each condition, 6-14 guts were imaged. The area

8   affected by tumors was measured using the measure function in ImageJ, and the average

9   proportion of the affected area for each gut was calculated.

10

11   ## Lysotracker staining, imaging and image analysis

12   Flies were immobilized on ice, dissected in PBS and stained with 0.5 µM Lysotracker DS

13   Red DND-99 (Invitrogen, Molecular Probes), containing 1:2000 0.5 mg/ml Hoechst 33342

14   (Sigma) for 3 min in 12-well plates on a shaker. Immediately after staining, guts were mounted

15   (Vectashield, H1000) and imaged using a Leica SP8-X confocal microscope. For each gut

16   preparation, an area proximal to the proventriculus was imaged to control for variation across

17   different gut regions, and 3 adjacent images per gut were captured. Images were analyzed

18   using IMARIS software. This experiment was carried out under blinded conditions.

19

20   ## LBP measurement in mouse plasma

21   Lipopolysaccharide-binding protein (LBP) was measured in mouse plasma samples by ELISA

22   according to the manufacturer's instructions (HyCult Biotech, HK: 205).

Transmission electron microscopy

The intestine was fixed in 2 % glutaraldehyde / 2 % formaldehyde in 0.1 M cacodylate buffer (pH 7.3) for 48 h at 4°C. Afterwards, samples were rinsed in 0.1 M cacodylate buffer (Applichem) and post-fixed with 2 % osmiumtetroxid (Science Services) in 0.1 M cacodylate buffer for 2 h at 4°C. Samples were dehydrated through an ascending ethanol series (Applichem) and embedded in epoxy resin (Sigma-Aldrich). Ultrathin sections (70 nm) were cut with a diamond knife (Diatome) on an ultramicrotome (EM-UC6, Leica Microsystems) and placed on copper grids (Science Services, 100mesh). The sections were contrasted with 1.5 % uranyl acetate (Plano) and lead citrate (Sigma-Aldrich). Images were acquired with a transmission electron microscope (JEM 2100 Plus, JEOL) and a OneView 4K camera (Gatan) with DigitalMicrograph software at 80 KV at RT. For each mouse and for each measured phenotype, 10 random images were taken and the final score for each mouse was calculated as a mean value obtained from 10 images. Imaging and scoring of EM data were carried out under blinded conditions.

Isolation of mouse intestinal crypts and organoid culture

Mouse jejunal section were used to isolate crypts according to the manufacturer's instructions (STEMCELL Technologies, document 28223). Complete IntestiCult medium was exchanged every 2-3 days and organoid numbers and *de novo* crypts were scored on days 5 and 7. This experiment was carried out under blinded conditions.

Immunostaining of mouse tissues

1 Jejunal sections were fixed in 4% PFA, embedded in paraffin and sectioned. Slides were

2 deparaffinized and antigen retrieval was performed by boiling with pH 6 citrate buffer. Primary

3 antibodies used were: p62/SQSTM (Abcam, 56416; 1:100), pH3 (CST, 4370; 1:100), lysozyme

4 (ThermoFisher Scientific, PA5-16668; 1:300), Man2B1 (St John's Laboratory, 640-850; 1:100).

5 Primary antibodies were detected using Alexa Flour 488-, Alexa Flour 594- and Alexa Flour 633-

6 conjugated anti-rabbit or anti-mouse secondary antibodies (Thermo Fisher Scientific, 1:500).

7 Sections were mounted in DAPI-containing mounting medium (Vectashield H-1200) and imaged

8 using confocal Leica SP8-DLS or SP8-X microscope.

9

10 **Metabolite extraction for lipid and polar metabolites from a single sample**

11 A fixed volume of 750 μL of a mixture of methanol: acetonitrile: water (40:40:20 [v:v]),

12 containing the appropriate internal standard (Everolimus, LC Laboratories) was added to the

13 samples. Samples were incubated for 30 min on an orbital shaker at 4°C followed by sonication

14 for 10 min in a cooled bath-type sonicator. Subsequently, samples were centrifuged for 10 min

15 at 16.000x g at 4°C and the supernatants were collected, while the insoluble pellet was dried by

16 aspirating the remaining liquid. 600 μL of chloroform: water (2:1 [v:v]) was added to the

17 collected supernatants and samples were mixed on the orbital shaker at 4°C for 10 min. Phases

18 were separated by centrifugation at 16.000x g and 4°C for 5 min. 500 μL of the upper, polar

19 phase and 500 μL of the lower, hydrophobic chloroform phase were collected and concentrated

20 in a speed vac concentrator.

21

22 **Rapamycin analysis by targeted UPLC-MS**

1   The concentrated chloroform-phase was resuspended in 50 µL of an

2   acetonitrile:isopropanol:DMSO [70:30:5 [v:v]) solution and the samples were sonicated for

3   5 min in a cooled bath-type sonicator. Insoluble components were removed by 10 min

4   centrifugation at 16000x g at 4°C and cleared supernatant was transferred to a fresh auto

5   sampler tube and used for the UPLC (Acquity i-class, Waters) -MS (TQ-S, Waters) analysis.

6   Chromatographic separation of 2 µL of the extract was performed using a 2.1 mm x 100 mm

7   BEH C8 column (Waters), using buffer A containing 10 mM ammonium acetate and 0.1% acetic

8   acid in water. Buffer B consisted of a mixture of 70:30 acetonitrile:isopropanol [v:v] containing

9   10 mM ammonium acetate and 0.1 % acetic acid. The gradient, which was carried out at a flow

10 rate of 300 µL/min was 0 min 55% A, 0.5 min 55 % A, 1.5 min 0 % A, 3.5 min 0 % A, 3.6 min 55 %

11 A and 6 min 55 % A. Samples were analysed by MRM analysis, monitoring the main adducts

12 (NH4) of Everolimus and Rapamycin. The selected transitions for each compound were m/z

13 931.78 → 864.64 and 931.78 → 882.64 for Rapamycin, while Everolimus was monitored using

14 transitions 975.65 → 908.5 and 975.65 → 926.5. Data analysis was performed using TargetLynx

15 XS.

16

17 **Peptide generation and TMT-labeling**

18 20 µL of lysis buffer (6 M GuCl, 2.5 mM TCEP, 10 mM CAA, 100 mM Tris-HCl) was added to

19 25 guts and tissues were homogenized using a hand-homogenizer. Homogenates were heated

20 at 95°C for 10 min and subsequently sonicated using the Bioruptor (10 cycles, 30 sec

21 sonication/30 sec break, high performance). Samples were centrifuged for 20 min at 2000x g

22 and supernatant was diluted 10-fold in 20 mM Tris. Protein concentration in the supernatant

1   was measured using a NanoDrop and 1:200 (w/w) of trypsin (Promega, Mass Spectrometry

2   grade) was added to 200 µg of sample. Trypsin digestion was performed overnight at 37°C and

3   stopped by the addition of 50% of formic acid (FA) to a final concentration of 1 %. Peptide

4   clean-up was carried out using an OASIS HLB Plate. Wetting of the wells was performed by the

5   addition of 200 µl of 60 % acetonitrile/0.1 % FA and equilibration adding 400 µl of 0.1 % FA. The

6   sample and 100 µl of 0.1 % FA were loaded into the wells and peptides eluted by the addition of

7   80 µl of 60 % ACN/0.1 % FA. Peptides were air-dried by using the SpeedVac and the pellet

8   resuspended in 60 µl of 0.1% FA. 15 µg of peptides was dried in SpeedVac and used for tandem

9   mass tag (TMT) labelling. The pellet was dissolved in 17 µl of 100 mM triethylammonium

10   bicarbonate (TEAB) and 41 µl of anhydrous acetonitrile was added. Samples were incubated for

11   10 min at RT with occasional vortexing, followed by the addition of 8 µl of TMT label and

12   subsequent incubation for 1 h at RT. The labelling reaction was stopped by the addition of 8 µl

13   of 5 % hydroxylamine and incubation for 15 min. Samples were air-dried in SpeedVac,

14   resuspended in 50 µl of 0.1 % FA and cleaned with an OASIS HLB Plate as previously described.

15   4 replicates per condition and 25 intestines per replicate were used for peptide generation and

16   TMT-labelling for proteomics analysis.

17

18   **High-pH fractionation**

19   Pooled TMT labeled peptides were separated on a 150 mm, 300 µm OD, 2 µm C18,

20   Acclaim PepMap (Thermo Fisher Scientific) column using an Ultimate 3000 (Thermo Fisher

21   Scientific). The column was maintained at 30°C. Buffer A was 5 % acetonitrile 0.01M ammonium

22   bicarbonate, buffer B was 80 % acetonitrile 0.01M ammonium bicarbonate. Separation was

1 performed using a segmented gradient from 1 % to 50 % buffer B, for 85 min and 50 % to 95 %

2 for 20 min with a flow of 4 μL. Fractions were collected every 150 sec and combined into nine

3 fractions by pooling every ninth fraction. Pooled fractions were dried in a Concentrator plus

4 (Eppendorf), resuspended in 5 μL 0.1% formic acid from which 2 μL was analyzed by LC-MS/MS.

5

6 LC-MS/MS analysis

7 Peptides from each of the nine high-pH fractions were separated on a 25 cm, 75 μm

8 internal diameter PicoFrit analytical column (New Objective) packed with 1.9 μm ReproSil-Pur

9 120 C18-AQ media (Dr. Maisch,) using an EASY-nLC 1200 (Thermo Fisher Scientific). The column

10 was maintained at 50°C. Buffer A and B were 0.1 % formic acid in water and 0.1 % formic acid in

11 80 % acetonitrile. Peptides were separated on a segmented gradient from 6% to 31% buffer B

12 for 120 min and from 31v% to 50 % buffer B for 10 min at 200 nl/min. Eluting peptides were

13 analyzed on an Orbitrap Fusion mass spectrometer (Thermo Fisher Scientific) in TMT-SPS mode.

14 Peptide precursor m/z measurements were carried out at 60000 resolution in the 350 to 1500

15 m/z range with an AGC target of 1e6. Precursors with charge state from 2 to 7 only were

16 selected for CID fragmentation using 35 % collision energy and an isolation window width of

17 0.7. The m/z values of the peptide fragments, MS/MS, were measured in the IonTrap at a

18 "Rapid" scan rate, a minimum AGC target of 1e4 and 100 ms maximum injection time. Upon

19 fragmentation, precursors were put on a dynamic exclusion list for 45 sec. The top ten most

20 intense MS/MS peaks were subjected to multi-notch isolation with an AGC target of 5e4 and

21 86 ms maximum injection time and further fragmented using HCD with 65 % collision energy.

1   The m/z values of the fragments, MS3, were measured in the Orbitrap at 50 K resolution. The

2   cycle time was set to two seconds.

3   Protein identification and quantification

4   The raw data were analyzed with MaxQuant version 1.5.2.8[46] using the integrated

5   Andromeda search engine[47]. Peptide fragmentation spectra were searched against the

6   canonical and isoform sequences of the *Drosophila melanogaster* reference proteome

7   (proteome ID UP000000803, downloaded September 2018 from UniProt). Methionine

8   oxidation and protein N-terminal acetylation were set as variable modifications; cysteine

9   carbamidomethylation was set as fixed modification. The digestion parameters were set to

10   "specific" and "Trypsin/P," The minimum number of peptides and razor peptides for protein

11   identification was 1; the minimum number of unique peptides was 0. Protein identification was

12   performed at peptide spectrum matches and protein false discovery rate of 0.01. The "second

13   peptide" option was on. The quantification type was set to "Reporter ion MS3" and "10-plex

14   TMT". Prior to the analysis, the TMT correction factors were updated based on the values

15   provided by the manufacturer.

16

17   <u>Bioinformatics</u>

18   Proteomics data analysis

19   Intensity values were log2 transformed and each sample was separately z-transformed.

20   For simpler interpretation the z-scores were rescaled to approximately their original scale by

21   multiplying each z-score with the overall standard deviation of the original log2 transformed

22   data and adding back the overall mean of the original log2 transformed data. The normalized

24

1   data were filtered for proteins that were detected in at least three replicates per biological

2   group and proteins annotated as contaminant or reverse identification were removed. Missing

3   values after filtering were imputed using the impute.knn function from the impute package

4   version 1.56.0[48]. Differential expression analysis was performed using the limma package

5   version 3.38.3[49]. P-values were corrected for multiple testing using the Benjamini-Hochberg

6   procedure and a significance threshold of 0.05 was used to determine significant differential

7   expression. Differential expression was determined between the following biological groups:

8   25-day old flies chronically treated with rapamycin vs. 25-day old control flies and 25-day old

9   flies treated with rapamycin from day 1-15 vs. 25-day old control flies. The normalized data

10   after batch effect removal with the removeBatchEffect function from the limma package was

11   used for principal component analysis using the prcomp function from the stats R package

12   version 3.5.3.

13

14   Gene ontology term enrichment

15   The topGO package version 2.32.0[50] with the annotation package org.dm.e.g.db[51] was

16   used for Gene ontology term enrichment analysis. The weight01 Fisher procedure[52] was used

17   with a minimal node size of five. The enrichment of each term was defined as the log2 of the

18   number of significant genes divided by the number of expected genes. Protein groups of

19   interest were tested for enrichment against a universe of all detected proteins. Only

20   significantly enriched terms with a minimum of three significant proteins and a maximum of

21   300 annotated genes were used in the cell plot

22

1   Statistical analyses

2   Statistical analysis was performed in GraphPad Prism except for survival analysis. Statistical

3   tests for each experiment are mentioned in the corresponding figure legends. Survival data

4   were analyzed with Log-rank test and Cox Proportional Hazard analysis, using Excel (Microsoft)

5   and Jmp (SAS Institute) software, respectively. Bioinformatics analysis was performed using R

6   (version 3.5.5).

7

Data Availability

9   The mass spectrometry proteomics data have been deposited to the ProteomeXchange

10   Consortium via the PRIDE partner repository with the dataset identifier PXD020820. Source

11   data are presented with the paper.

12

Acknowledgments

26

5

Author contributions

7   P.J. and L.P. conceptualized study, P.J., S.G., Y.X.L., T.L. and L.P. designed the experiments, P.J.,

8   Y.X.L., T.L., L.F.D., J.L., T.N., S.A., J.C.R., E.F. and J. F. conducted the experiments, P.J., Y.X.L., T.L.

9   analyzed the data, J.P. analyzed the proteomics data, P.J., S.G. and L.P. wrote original

10   manuscript, P.J., Y.X.L., S.G. and L.P. edited it, P.J., Y.X.L. and T.L. contributed equally.

11

Competing interests

13   Authors declare no competing interests.

14

References

1   Robida-Stubbs, S. *et al.* TOR signaling and rapamycin influence longevity by regulating SKN-1/Nrf and DAF-16/FoxO. *Cell metabolism* **15**, 713-724, doi:10.1016/j.cmet.2012.04.007 (2012).

2   Bjedov, I. *et al.* Mechanisms of life span extension by rapamycin in the fruit fly Drosophila melanogaster. *Cell metabolism* **11**, 35-46, doi:10.1016/j.cmet.2009.11.010 (2010).

3   Harrison, D. E. *et al.* Rapamycin fed late in life extends lifespan in genetically heterogeneous mice. *Nature* **460**, 392-395, doi:10.1038/nature08221 (2009).

4   Halloran, J. *et al.* Chronic inhibition of mammalian target of rapamycin by rapamycin modulates cognitive and non-cognitive components of behavior throughout lifespan in mice. *Neuroscience* **223**, 102-113, doi:10.1016/j.neuroscience.2012.06.054 (2012).

5   Anisimov, V. N. *et al.* Rapamycin increases lifespan and inhibits spontaneous tumorigenesis in inbred female mice. *Cell Cycle* **10**, 4230-4236, doi:10.4161/cc.10.24.18486 (2011).

6   Dai, D. F. *et al.* Altered proteome turnover and remodeling by short-term caloric restriction or rapamycin rejuvenate the aging heart. *Aging cell* **13**, 529-539, doi:10.1111/acel.12203 (2014).

7   Flynn, J. M. *et al.* Late-life rapamycin treatment reverses age-related heart dysfunction. *Aging cell* **12**, 851-862, doi:10.1111/acel.12109 (2013).

8   Chen, C., Liu, Y., Liu, Y. & Zheng, P. mTOR regulation and therapeutic rejuvenation of aging hematopoietic stem cells. *Sci Signal* **98** (2009).

9   Lamming, D. W. *et al.* Rapamycin-Induced Insulin Resistance Is Mediated by mTORC2 Loss and Uncoupled from Longevity. *Science* **335**, 1638-1643 (2012).

10 Wilkinson, J. E. *et al.* Rapamycin slows aging in mice. *Aging Cell* **11**, 675-682 (2012).

11 Bitto, A. *et al.* Transient rapamycin treatment can increase lifespan and healthspan in middle-aged mice. *Elife* **5**, e16351, doi:10.7554/eLife.16351 (2016).

12 Arriola Apelo, S. I., Pumper, C. P., Baar, E. L., Cummings, N. E. & Lamming, D. W. Intermittent Administration of Rapamycin Extends the Life Span of Female C57BL/6J Mice. *J Gerontol A Biol Sci Med Sci* **71**, 876-881, doi:10.1093/gerona/glw064 (2016).

13 Mannick, J. B. *et al.* mTOR inhibition improves immune function in the elderly. *Sci Transl Med* **6**, a179 (2014).

14 Mannick, J. B. *et al.* TORC1 inhibition enhances immune function and reduces infections in the elderly. *Sci Transl Med* **10**, eaaq1564 (2018).

15 Biteau, B. *et al.* Lifespan extension by preserving proliferative homeostasis in Drosophila. *PLoS genetics* **6**, e1001159, doi:10.1371/journal.pgen.1001159 (2010).

16 Fan, X. *et al.* Rapamycin preserves gut homeostasis during Drosophila aging. *Oncotarget* **6**, 35274-35283, doi:10.18632/oncotarget.5895 (2015).

17 Hans, F. & Dimitrov, S. Histone H3 phosphorylation and cell division. *Oncogene* **20**, 3021-3027 (2001).

18   Jiang, H., Grenley, M. O., Bravo, M. J., Blumhagen, R. Z. & Edgar, B. A. EGFR/Ras/MAPK signaling mediates adult midgut epithelial homeostasis and regeneration in Drosophila. *Cell Stem Cell* **8**, 84-95, doi:10.1016/j.stem.2010.11.026 (2011).

19   Liang, J., Balachandra, S., Ngo, S. & O'Brien, L. E. Feedback regulation of steady-state epithelial turnover and organ size. *Nature* **548**, 588-591, doi:10.1038/nature23678 (2017).

20   Salazar, A. M. *et al.* Intestinal Snakeskin Limits Microbial Dysbiosis during Aging and Promotes Longevity. *iScience* **9**, 229-243, doi:10.1016/j.isci.2018.10.022 (2018).

21   Lu, Y. X. *et al.* A TORC1-histone axis regulates chromatin organisation and non-canonical induction of autophagy to ameliorate ageing. *eLife* **10**, doi:10.7554/eLife.62233 (2021).

22   Ulgherait, M., Rana, A., Rera, M., Graniel, J. & Walker, D. W. AMPK modulates tissue and organismal aging in a non-cell-autonomous manner. *Cell Rep* **8**, 1767-1780, doi:10.1016/j.celrep.2014.08.006 (2014).

23   Cadwell, K. *et al.* A key role for autophagy and the autophagy gene Atg16l1 in mouse and human intestinal Paneth cells. *Nature* **456**, 259-263, doi:10.1038/nature07416 (2008).

24   Bel, S. *et al.* Paneth cells secrete lysozyme via secretory autophagy during bacterial infection of the intestine. *Science* **357**, 1047-1052, doi:10.1126/science.aal4677 (2017).

25   Cani, P. D. *et al.* Changes in gut microbiota control metabolic endotoxemia-induced inflammation in high-fat diet-induced obesity and diabetes in mice. *Diabetes* **57**, 1470-1481, doi:10.2337/db07-1403 (2008).

26   Ott, B. *et al.* Effect of caloric restriction on gut permeability, inflammation markers, and fecal microbiota in obese women. *Sci Rep* **7**, 11955, doi:10.1038/s41598-017-12109-9 (2017).

27   Ma, T. Y., Hollander, D., Dadufalza, V. & Krugliak, P. Effect of aging and caloric restriction on intestinal permeability. *Exp Geront* **27**, 321-333 (1992).

28   Parikh, K. *et al.* Colonic epithelial cell diversity in health and inflammatory bowel disease. *Nature* **567**, 49-55, doi:10.1038/s41586-019-0992-y (2019).

29   Zhao, M. *et al.* Deficiency in intestinal epithelial O-GlcNAcylation predisposes to gut inflammation. *EMBO Mol Med* **10**, e8736, doi:10.15252/emmm.201708736 (2018).

30   Söderholm, J. D. *et al.* Augmented increase in tight junction permeability by luminal stimuli in the non-inflamed ileum of Crohn's disease. *Gut* **50**, 307-313, doi:10.1136/gut.50.3.307 (2002).

31   Clevers, H. C. & Bevins, C. L. Paneth cells: maestros of the small intestinal crypts. *Annu Rev Physiol* **75**, 289-311, doi:10.1146/annurev-physiol-030212-183744 (2013).

32   Yilmaz, O. H. *et al.* mTORC1 in the Paneth cell niche couples intestinal stem-cell function to calorie intake. *Nature* **486**, 490-495, doi:10.1038/nature11163 (2012).

33   Adolph, T. E. *et al.* Paneth cells as a site of origin for intestinal inflammation. *Nature* **503**, 272-276, doi:10.1038/nature12599 (2013).

34   Pentinmikko, N. *et al.* Notum produced by Paneth cells attenuates regeneration of aged intestinal epithelium. *Nature* **571**, 398-402, doi:10.1038/s41586-019-1383-0 (2019).

35   Huang, J. & Klionsky, D. J. Autophagy and human disease. *Cell Cycle* **6**, 1837-1849, doi:10.4161/cc.6.15.4511 (2007).

36   Hara, T. *et al.* Suppression of basal autophagy in neural cells causes neurodegenerative disease in mice. *Nature* **441**, 885-889, doi:10.1038/nature04724 (2006).

37   Slack, C. *et al.* The Ras-Erk-ETS-Signaling Pathway Is a Drug Target for Longevity. *Cell* **162**, 72-83, doi:10.1016/j.cell.2015.06.023 (2015).

38   Guo, L., Karpac, J., Tran, S. L. & Jasper, H. PGRP-SC2 promotes gut immune homeostasis to limit commensal dysbiosis and extend lifespan. *Cell* **156**, 109-122, doi:10.1016/j.cell.2013.12.018 (2014).

39   Mathur, D., Bost, A., Driver, I. & Ohlstein, B. A Transient Niche Regulates the Specification of Drosophila Intestinal Stem Cells. *Science* **327**, 210-213 (2010).

40   Regan, J. C. *et al.* Sex difference in pathology of the ageing gut mediates the greater response of female lifespan to dietary restriction. *Elife* **5**, e10956, doi:10.7554/eLife.10956 (2016).

41   Ren, C., Finkel, S. E. & Tower, J. Conditional inhibition of autophagy genes in adult Drosophila impairs immunity without compromising longevity. *Experimental gerontology* **44**, 228-235, doi:10.1016/j.exger.2008.10.002 (2009).

42   Scott, R. C., Schuldiner, O. & Neufeld, T. P. Role and regulation of starvation-induced autophagy in the Drosophila fat body. *Developmental cell* **7**, 167-178, doi:10.1016/j.devcel.2004.07.009 (2004).

43   Tain, L. S. *et al.* Tissue-specific modulation of gene expression in response to lowered insulin signalling in Drosophila. *eLife* **10**, doi:10.7554/eLife.67275 (2021).

44   Bass, T. M. *et al.* Optimization of Dietary Restriction Protocols in Drosophila. *J Gerontol A Biol Sci Med Sci* **62**, 1071-1081 (2015).

45   Nagy, P., Varga, Á., Kovács, A. L., Takáts, S. & Juhász, G. How and why to study autophagy in Drosophila: It's more than just a garbage chute. *Methods* **75**, 151-161, doi:10.1016/j.ymeth.2014.11.016 (2015).

46   Cox, J. & Mann, M. MaxQuant enables high peptide identification rates, individualized p.p.b.-range mass accuracies and proteome-wide protein quantification. *Nat Biotechnol* **26**, 1367-1372, doi:10.1038/nbt.1511 (2008).

47   Cox, J. *et al.* Andromeda: a peptide search engine integrated into the MaxQuant environment. *J Proteome Res* **10**, 1794-1805, doi:10.1021/pr101065j (2011).

48   Hastie, T., Tibshirani, R., Narasimhan, B. & Chu, G. impute: Imputation for microarray data. R package version 1.56.0. (2019).

49   Phipson, B., Lee, S., Majewski, I. J., Alexander, W. S. & Smyth, G. K. Robust Hyperparameter Estimation Protects against Hypervariable Genes and Improves Power to Detect Differential Expression. *Ann Appl Stat* **10**, 946-963, doi:10.1214/16-AOAS920 (2016).

50   Alexa, A. & Rahnenfuhrer, J. topGO: Enrichment Analysis for Gene Ontology. R package version 2.32.0. (2019).

51   Carlson, M. org.Dm.eg.db: Genome wide annotation for Fly. R package version 3.7.0. (2019).

52   Alexa, A., Rahnenfuhrer, J. & Lengauer, T. Improved scoring of functional groups from gene expression data by decorrelating GO graph structure. *Bioinformatics* **22**, 1600-1607, doi:10.1093/bioinformatics/btl140 (2006).
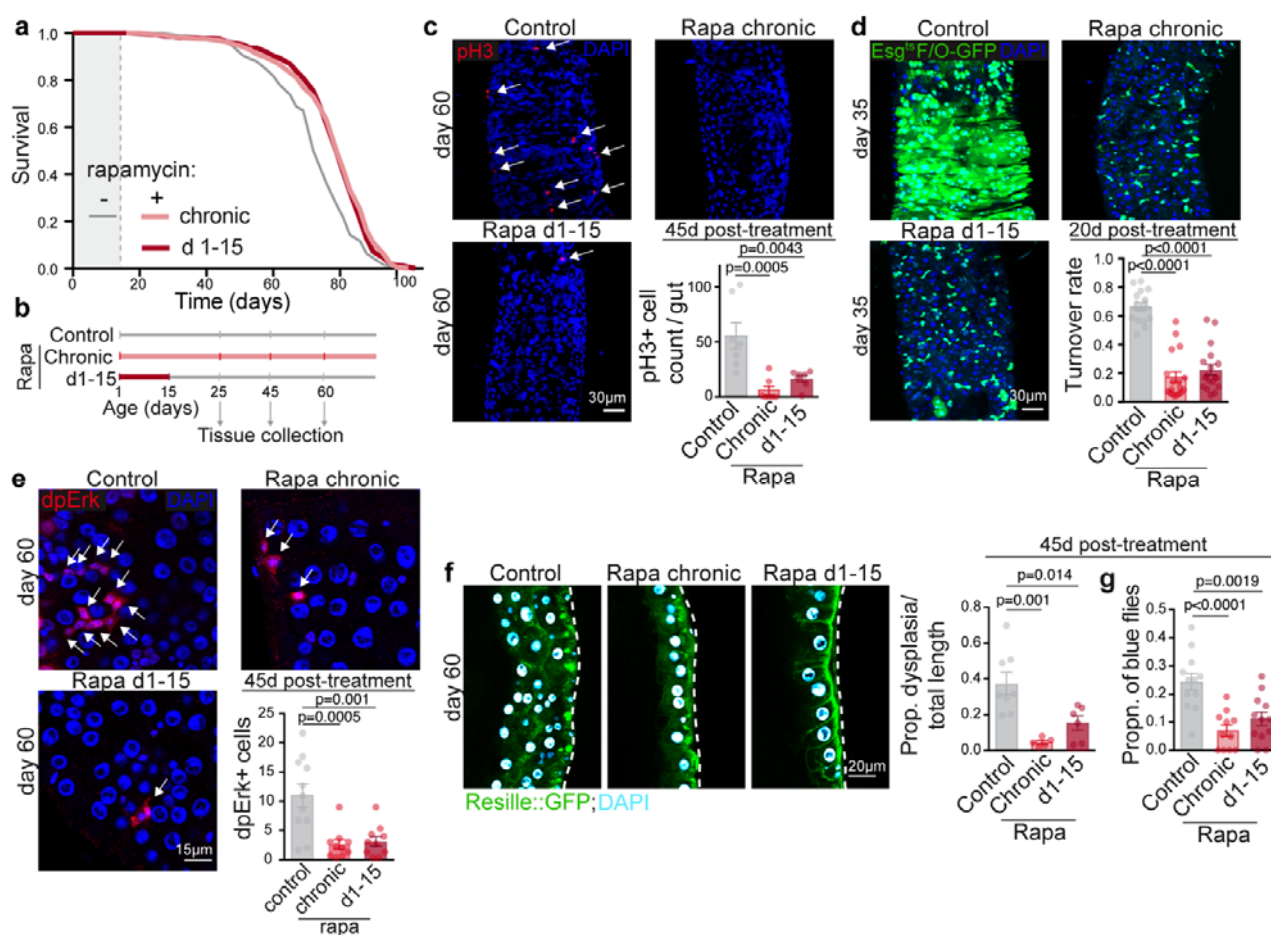
Main Figures

Fig. 1: Brief rapamycin treatment early in adulthood extends lifespan and preserves intestinal function as much as does chronic treatment.

a, Lifespan of flies chronically or in days 1-15 treated with rapamycin (n=400 per condition, see also Extended Data Table 3). **b**, Experimental design. **c**, The number of pH3+ cells (arrows) in the gut 45 days after the short-term rapamycin treatment was withdrawn (n=7-8). **d**, Midgut turnover rate, as assessed with the esg^{ts}F/O system 20 days post-treatment (n=15-18). **e**, The number of dpErk+ cells 45-days post-rapamycin treatment (n=10-11). **f**, Intestinal dysplasia in gut R2 region of flies carrying epithelial marker Resille-GFP 45-days after short-term rapamycin treatment was terminated (n=6-8). **g**, Intestinal barrier function in flies treated with rapamycin chronically or in days 1-15. Data are mean ± s.e.m. One-way ANOVA, Bonferroni's post-test.
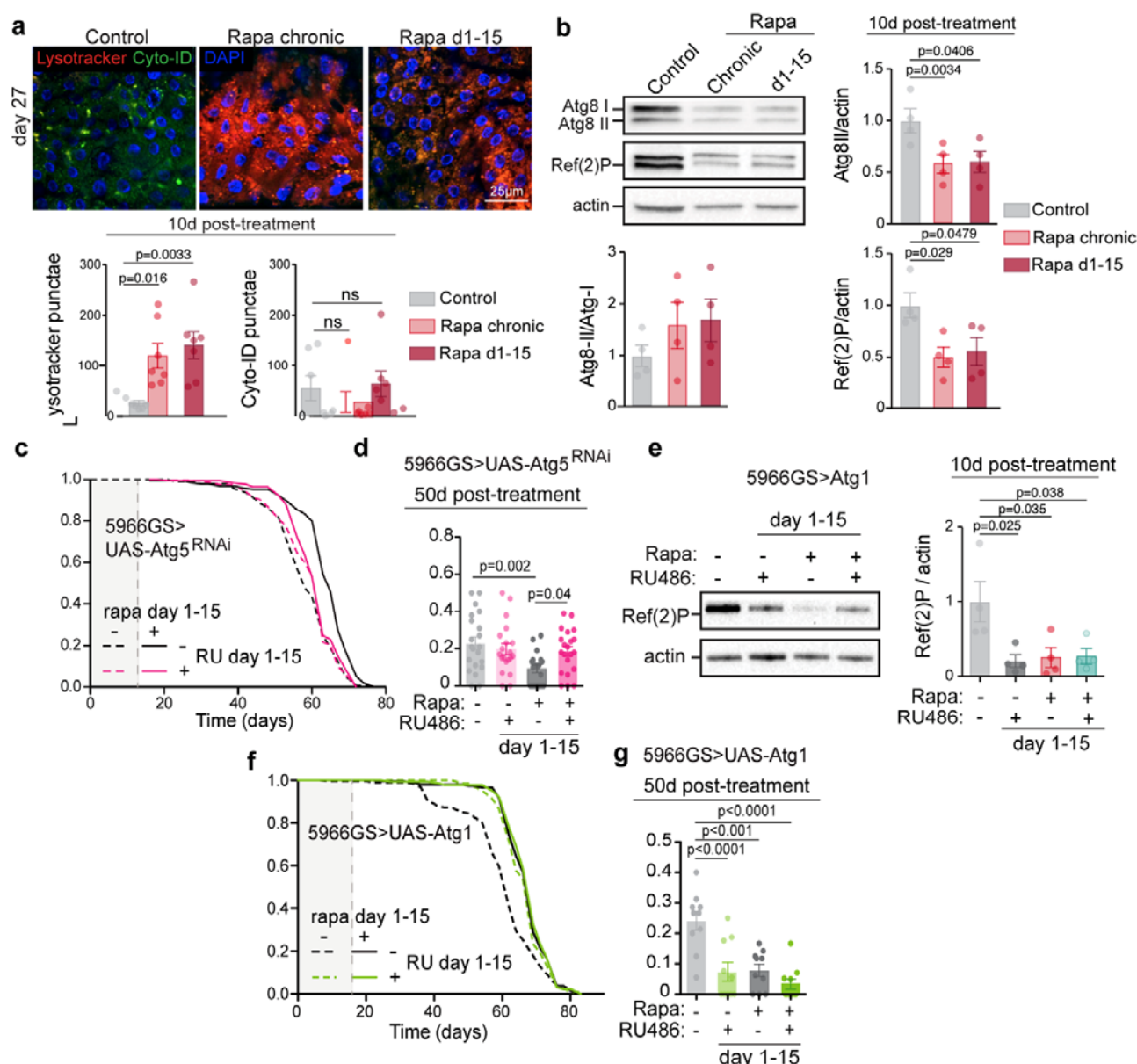
Fig. 2: Short-term rapamycin treatment or *Atg1* over-expression induces lasting autophagy activation.

a, Number of punctae stained by LysoTracker and Cyto-ID in 25-day old flies chronically or in days 1-15 treated with rapamycin (n=7). b, Immunoblot of autophagy-related proteins, Atg8-I, Atg8-II and Ref-2-P in the fly gut on day 25, 10-days post-rapamycin-treatment (n=4). c, Rapamycin extended lifespan of control flies (p=8.8 x 10^{-10}) but not of flies expressing RNAi against Atg5 in enterocytes in days 1-15 (p=0.097, n=400, see also Extended Data Table 5). d, Rapamycin reduced the proportion of blue flies in control group, but not in flies expressing enterocyte-specific *Atg5*-RNAi. Rapamycin*genotype interaction (p=0.020). e, Immunoblot of intestinal Ref-2-P of flies treated with rapamycin from day 1-15 in combination with enterocyte-specific over-expression of Atg1 in days 1-15, measured 10 days post-treatment (n=4). Genotype*rapamycin interaction (p=0.03). f, Day 1-15 over-expression of *Atg1* specifically in enterocytes extended lifespan (p=6.7 x 10^{-05}) to the same degree as rapamycin (p=0.69, see also Extended Data Table 7). N=160-200. Log rank test and CPH. g, Over-expression of *Atg1* in days 1-15 reduced the proportion of blue flies to the same degree as rapamycin treatment. Rapamycin*genotype interaction for chronic (p=0.02). n=10 vials per condition with 20 flies per vial. Data are mean ± s.e.m. One-way (a-b) or Two-way (d-g) ANOVA; Bonferroni's multiple comparison test.
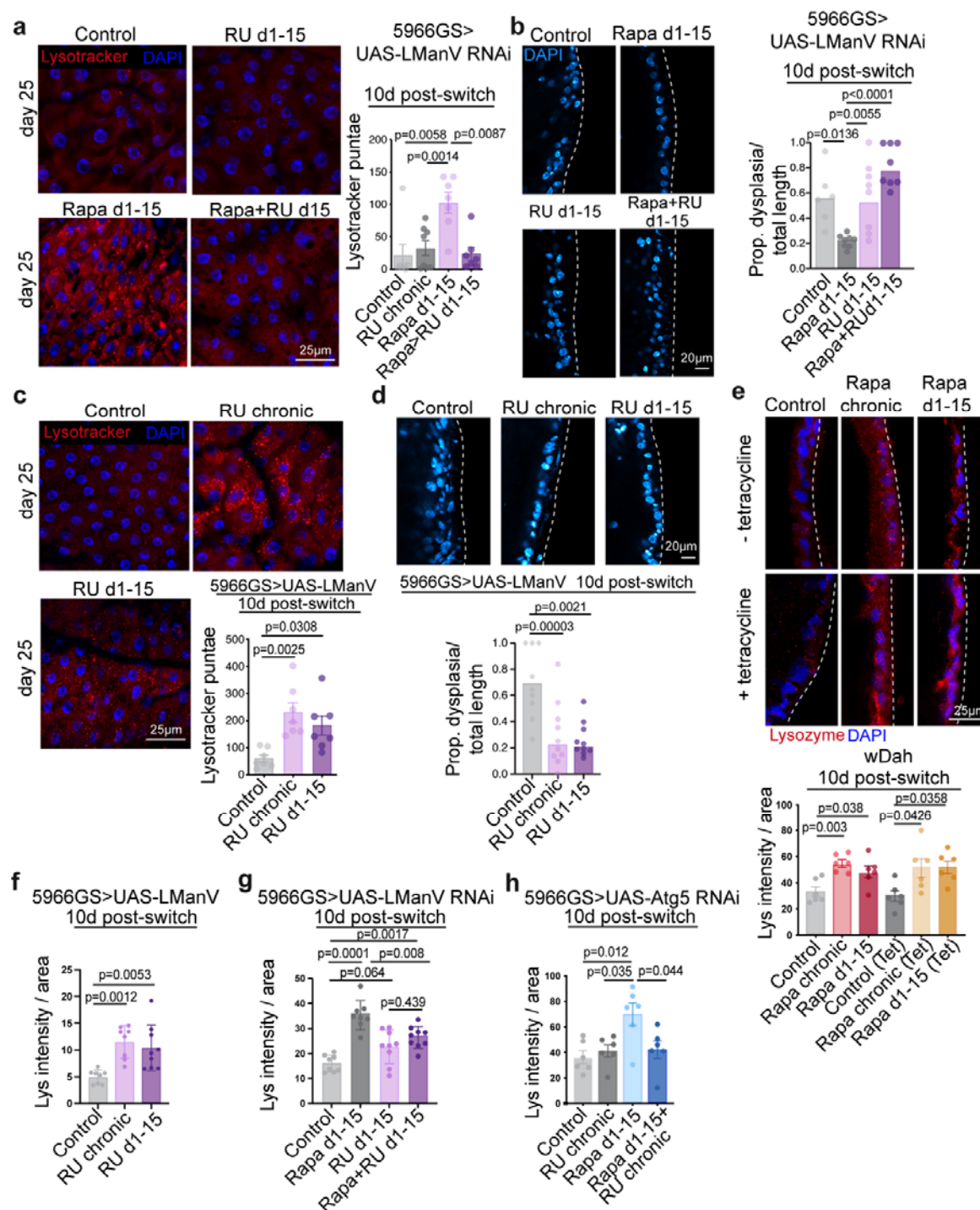
Fig. 3: Persistent increase in LManV mediates the "memory of autophagy" and reduced age-related gut pathology induced by short-term rapamycin treatment. a-b, Over-expression of RNAi against LManV in enterocytes in days 1-15 abolished increase in lysotracker staining (**a**) and reduction in gut pathology (**b**) induced by short-term rapamycin treatment. **c-d,** Over-expression of LManV in enterocytes in days 1-15 increased lysotracker staining (**c**) and reduced age-related gut-pathology (**d**) to the same degree as chronic over-expression of LManV. **e,** Chronic and short-term rapamycin treatment increased intestinal lysozyme level irrespective of tetracycline treatment. **f,** Chronic and short-term over-expression of LManV increased lysozyme to the same degree. **g,** Over-expression of RNAi against LManV in enterocytes in days 1-15 abolished increase in lysozyme induced by rapamycin treatment in days 1-15. **h,** Over-expression of RNAi against Atg5 in enterocytes in days 1-15 abolished increase in lysozyme induced by rapamycin treatment in days 1-15.
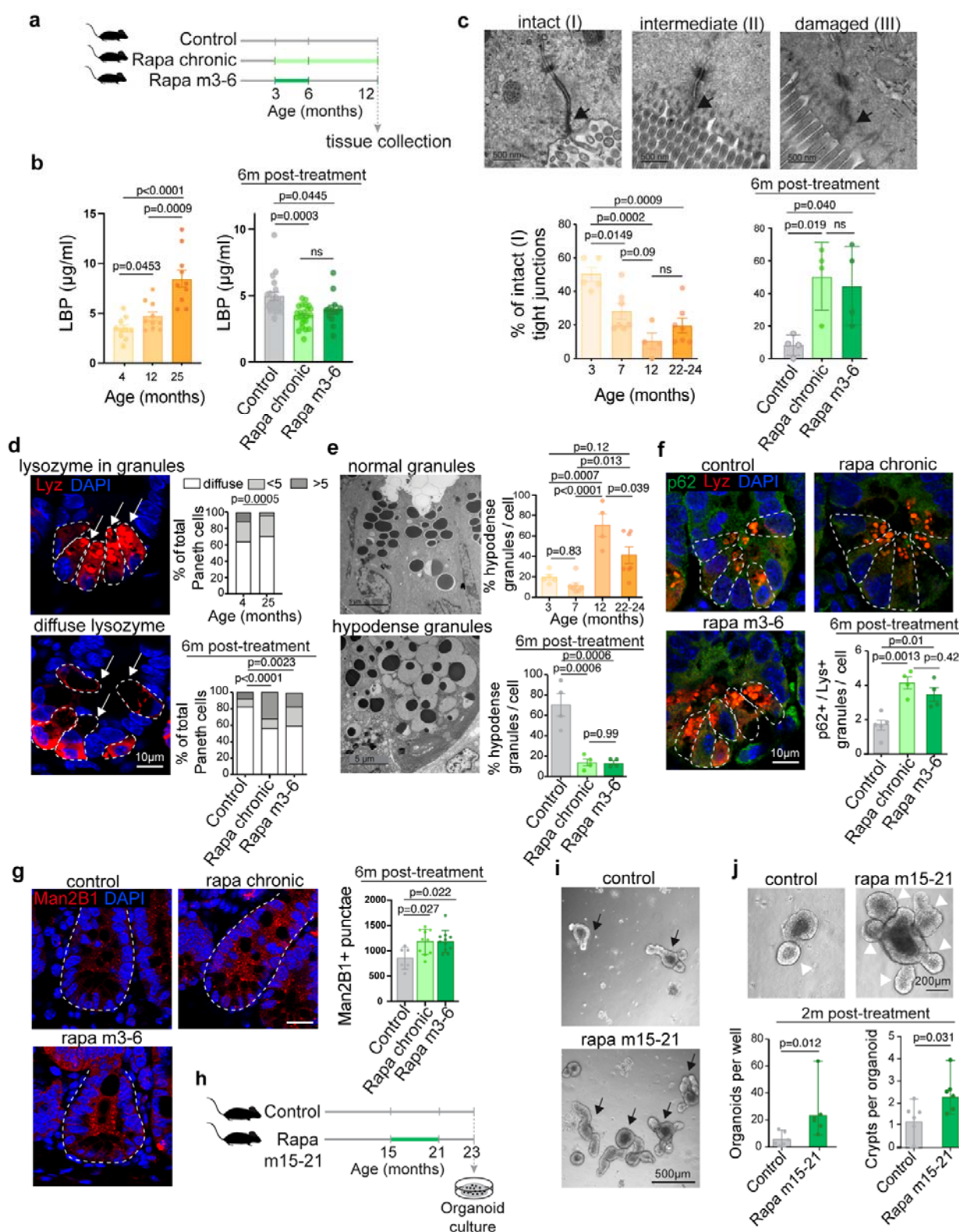
Fig. 4: Short-term rapamycin exposure maintains gut barrier function, Paneth cell architecture and regenerative capacity of ISCs to the same degree as lifelong treatment in mice.

a, Experimental design. b, Plasma LBP levels during ageing and 6 months after rapamycin treatment was terminated (n=10-15 mice). c, Tight junction pathology score: I - narrow and electron dense TJs; II - reduced electron density, but no dilations within TJs; III - low electron density and dilated TJs. Proportion of intact TJs during ageing and 6 months post-rapamycin-treatment. d, The proportion of Paneth cells with diffuse lysozyme staining was increased in aged mice and rapamycin reduced the proportion of Paneth cells (arrows) with diffuse lysozyme staining, which remained reduced 6 months post-treatment (n=4). e,

Proportion of hypodense Paneth cell granules in mouse jejunum during ageing and 6 months after rapamycin treatment was withdrawn. **f**, The number of lysozyme+/p62+ granules per Paneth cell was increased by rapamycin and remained increased 6 months after the treatment was withdrawn (n=4). White dashed denotes a Paneth cell. **g**, Number of Man2B1+ punctae was increased by rapamycin and remained increased 6-months post-treatment. White dashed denotes a crypt unit. One-way ANOVA; Bonferroni's multiple comparison test. **h**, Experimental design. **i**, Rapamycin increased organoid forming potential of intestinal crypts (arrows) and (**j**), formation of de novo crypts (white arrowheads), which remained increased 2 months post-treatment (n=6).